



SCIENTIA
IRANICA

Sharif University of Technology

Scientia Iranica

Transactions D: Computer Science & Engineering and Electrical Engineering

<https://scientiairanica.sharif.edu>



Introducing a new shimming method based on combination of axial and radial Halbach arrays to have a uniform flux density for a low-field portable MRI system

Mohammadreza Shiravi and Babak Ganji*

Faculty of Electrical and Computer Engineering, University of Kashan, P.O.Box 87317-51167, Kashan, Iran.

Received 11 June 2021; received in revised form 1 June 2023; accepted 8 August 2023

KEYWORDS

Halbach magnet;
Shimming;
Inhomogeneity;
Magnetic Resonance
Imaging (MRI);
Optimization.

Abstract. Nowadays, Halbach magnets serve different purposes in electrical machine designs by offering different structures. These structures can be used to shim (improve the inhomogeneity) of new static fields in the Magnetic Resonance Imaging (MRI) system. The shimming method proposed here uses axial and radial Halbach arrays. The inhomogeneity and average field is obtained at a constant diameter of spherical volume. Using the Maxwell software, different topologies are evaluated and the best structure is then selected and optimized. The optimum structure is manufactured and all issues related to the construction are explained in details. Comparison between simulation and experimental results shows the effectiveness of the proposed idea.

© 2024 Sharif University of Technology. All rights reserved.

1. Introduction

In our previous research, an H-type magnet with an iron core was made [1]. For this structure, simple shimming and optimization are its advantages. However, disadvantages were heavy, expensive and time consuming to build. Because of these disadvantages, research is focused on Halbach magnets. Halbach's

theory was first proposed by Halbach in 1979 [2]. By this theory, different types of static fields and magnets are classified. To create a bipolar field (in Halbach's theory $m = 2$), according to the need for the size of the field density, its uniformity and mass weight, various structures can be implemented. Using a permanent magnet (PM) with axial polarity (including cubic PM) and radial polarity (including ideal ring, cylindrical pieces, with hexagonal cross-section, and sectional cross-section), the Halbach magnet is made. By changing the number of PM pieces and the distance

*. Corresponding author.

E-mail address: bganji@kashanu.ac.ir (B. Ganji)

To cite this article:

M. Shiravi, and B. Ganji "Introducing a new shimming method based on combination of axial and radial Halbach arrays to have a uniform flux density for a low-field portable MRI system", *Scientia Iranica* (2024), **31**(21), pp. 1971-1980

<https://doi.org/10.24200/sci.2023.58266.5647>

between the radial and axial rings, the magnitude and uniformity of the field can be improved.

In recent years, many works have been done on the Halbach magnet issue. A comprehensive study of the primitive Magnetic Resonance Imaging (MRI) system is done in [3] and information about the selection of component such as PMs is also provided. In [4], gradient coils are designed and produced based on the shape and type of the Halbach magnetic field. In [5], the structure of the Halbach magnet (the radius of each Halbach layer) is optimized by using the genetic algorithm (GA) in the distributed evolutionary algorithms in Python (DEAP). In [6], the effect of changing the angle of the PM dipoles of the Halbach ring for controlling the magnetic field density is investigated. In [7], a portable MRI system has been launched. All components such as MRI console, static magnet, gradient coil and RF coil are prepared and then installed. In [8], optimal location of each cubic PM piece to have the desired uniformity in the field is obtained by GA. In [9], the effect of temperature increase on the hysteresis curve and the operating point of the PM piece has been practically investigated. In [10], a purely theoretical discussion of the optimization of the Halbach machine field using GA has been proposed. Accordingly, Halbach array segments with different arc lengths are used to obtain the maximum field. In [11], the gradient coils and its amplifier circuit are designed and built according to the structure of the Halbach magnet array.

Two different designs are produced in [12]. At first, Halbach magnet is combined from two main rings with a gap between them (this gap is optimized) and two shim rings is installed inside the main rings. Main rings consist of 2 pcs with 12-cylinder PM which are distributed along a circle. The height of Halbach magnet and the gap between two rings are optimized. Regarding the Shim rings, the height and the radius of shim magnets must be optimized. Another design is also considered in this reference: two main rings including 2 pcs with 16-cylinder PM. The radius, length of Halbach magnet and the gap between two rings are optimized. Two shim rings including 8 PM pieces are also considered and height of position of shim rings are optimized. In [13], the Halbach magnet consists of four rings. Gap between each ring is known. The radius and height of Halbach magnet are also known. Each ring includes 24 pcs cubic PM. In [14], very small hexagonal bar magnets were used for constructing Halbach magnet. In [15], Halbach magnet is produced from two nested continued rings. Each ring was combined from 16 PM pieces. In this state, there are three types of polarization. By rotation inside ring or outside ring from 0° to 180° , the field is changed from $B_1 + B_2$ to $B_1 - B_2$. In [16], two radially polarized outward magnet rings are analyzed. The configuration of these rings is changed based on the optimization

algorithm to generate a homogenous field in region of interest (ROI).

In [17], magnet ring is made by 12 PM sections. Inner radius, outer radius and height of ring are known. In [18], both circular array and cylinder array are produced. The radius of circular array is known and consists of 48 pcs cubic PMs. Harness is made from Poly Methyl Metha Acrylate (PMMA) by a laser cutter. In [19], the radius of Halbach ring is known and is combined from 20 PM elements with known dimensions as well as two end-magnet rings consisting of 20 pcs magnet cubes placed along a calculated radius circle. Harness is made from polyamide and its radius is obtained. In [20], the Halbach magnet consists of two rings of 24 pcs cubic PM that is distributed along a known circular ring. Harness was made by 3D printer from Poly Lactic Acid (PLA) material. In [21], common configuration is used and Magnet Arrangement for Novel Discrete Halbach Layout (MANDHaLa) is composed of cubic PMs. Four Halbach rings are used where the gap between rings is known. The radius and length of whole magnet are also known. Each ring is made from 24 N52 NdFeB cubes. Special attention has been paid to use of the Halbach magnet for the MRI system in recent years [22-23]. In present paper, a new shimming method based on the Halbach magnet is introduced for the MRI system to improve average field and homogeneity. Simulation and construction of the proposed idea is also considered. In the following, the proposed method is introduced in Section 2. Simulation and experimental results are given in Sections 3 and 4, respectively. Finally, the paper is concluded in Section 5.

2. The proposed method

The main idea is that Halbach array is a shimming structure. This can also shim its inhomogeneity. In other words, research on the Halbach magnet puts endless ideas in front of the researcher to solve non-uniformity problems. First, we consider C-type, H-type, and U-type static magnets. As indicated above, it is possible to correct their inhomogeneity using Halbach configuration. It means that PM pieces should be installed radially inside the main magnet or axially near the previous magnet that their polarity, position of rotation, and volume (cross section and thickness) is obtained by Halbach array geometry equations. The volume of PM pieces is also proportional to our design that would be obtained by optimization algorithms or via trial-and-error method.

For producing a homogenous field, three methods can be used which are described in the following:

1. Numerical method:

Magnetic field is produced by a magnetic

dipole [24]:

$$B = \frac{\mu_0}{4\pi} \frac{3(Mr)r - r^2 M}{r^5}, \quad (1)$$

where $\vec{M} = \vec{m}V$, m is the magnetizing intensity, $\vec{H} = \vec{B}/\mu_0 + \vec{M} \xrightarrow{H=0} m = -B_r/\mu_0$ and it can be positive or negative depending on its direction, $V = tS$, S is the magnet area. Then, $t = \mu_0 M/(B_r S)$. The alteration of B_r and thickness (t) and cross section (S) of PM pieces can shape the homogeneity of field. The location of PM pieces can be determined using Halbach approach, $r = (x_k - x_p, y_k - y_p, z_k - z_p)$ where $k = 1, \dots, N_s$ is used for shimming blocks or effect of k th PM piece and $p = 1, \dots, N$ is used for test points. The parameter B will be homogenous if one of its three components will be homogenous. Then, $B_z^k(r_p)$ is used for homogenous research [25]:

$$B_z(r_p, r_k) = \frac{\mu_0 M_k}{4\pi} \frac{2(z_p - z_k)^2 - (x_p - x_k)^2 - (y_p - y_k)^2}{(r_p - r_k)^5}. \quad (2)$$

Eq. (2) is equal to $A_{p,k} V_k m_z$ that $A_{p,k} \in A$ is a non-square transformer matrix. Then, $M = A^T (A A^T)^{-1} B$ and volume (V) and thickness (t) of PM pieces are obtained.

2. Optimization algorithms:

Using evolutionary algorithms such as GA and particle swarm optimization (PSO) algorithms, objective function could be minimized as follows:

$$OF = \sum_{p=1}^N \left(B_p - B_{avg} - \sum_{k=1}^{N_s} B_{p,k} \right)^2 + \alpha \sum_{k=1}^{N_s} V_k^2, \quad (3)$$

where B_p is the initial field at each testing point and B_{avg} is the average field in the ROI. And, $\alpha = 0$ means the goal is to minimize inhomogeneity.

3. The trial-and-error method:

For our desired field, Halbach magnet is designed using Maxwell software. The field uniformity of ROI is then calculated in the different states (different gap, different shim size and number) as follows:

$$\eta = \frac{B_{\max} - B_{\min}}{B_{avg}} \times 10^6, \quad (4)$$

where its unit is parts-per-million (ppm), B_{\max} , B_{\min} and B_{avg} are respectively maximum, minimum, and average of magnetic field density in the ROI. Also, three performance factors should be calculated to evaluate magnet array. First: $F_B = B_{avg}/\eta$, second: $F_A = F_B/S$ and third: $F_\omega = \omega^{7/4}/(\eta_S)$ where, Larmor frequency is ω and area of PM magnet is S (cm²) [26]. Next, for magnet suitability and compactness of MRI,

a figure of merit \mathfrak{R} (T/kg) has been defined ($\mathfrak{R} = F_B \times (V_S/\rho V^2)$) [14]. The mass density of magnet is ρ and the volume of sample and magnet are V_S and V , respectively.

For all three above-mentioned methods, the Halbach magnet should be analyzed: Magnetization of linear Halbach array is followed by Eq. (5) and flux is oscillated with a wavelength $\lambda = 2\pi/k$ in x coordinate direction. When the wavelength is bent to a circle, magnetization is then followed by Eq. (6). For dipole Halbach ($j = \pm 1$), and for quadrupole ($j = \pm 2$) and so on, the details are presented in [15]. In Figure 1, α_i is the position angle of i th PM piece, β_i denotes the magnetization angle of i th PM piece, $i = 1, \dots, n-1$ and n is the number of PM pieces. These parameters have been used in Eq. (7). Circle diameter of PM piece is a and r_{in} , r_{out} and r_d are inner radius of cylindrical magnet, outer radius of cylindrical magnet, and $(r_{in} + r_{out})/2$, respectively. In Table 1, these parameters have been achieved by Eqs. (8)-(10). For donut Halbach ring with infinitely length, B is obtained from Eq. (11). And, B_r is remanence of the magnetic material. It should be noted that all these equations have been proven for cubic PM pieces in [26].

$$M(x) = \begin{pmatrix} M_t \\ M_n \end{pmatrix} = M_0 \begin{pmatrix} \sin kx \\ \cos kx \end{pmatrix}, \quad (5)$$

where M_t is the tangential component and M_n is the normal component [26].

$$M(r, \alpha) = M_0 \begin{pmatrix} \sin \beta \\ \cos \beta \end{pmatrix}, \beta = (1 + j)\alpha, j \in \mathbb{Z}, \quad (6)$$

$$\alpha_i = \frac{2\pi i}{n}, \beta_i = 2\alpha_i. \quad (7)$$

Equations for the dimensions of the Halbach magnet for cubic and cylindrical PM parts are as follows [24]:

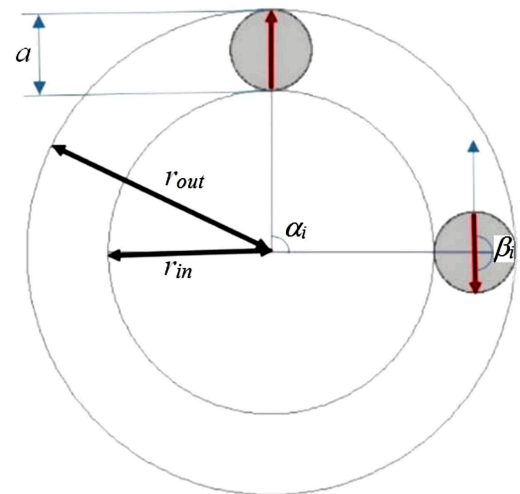


Figure 1. The position angle α_i and angle of dipole rotation β_i in the Halbach magnet.

Table 1. Homogeneity analysis of Halbach rings (with 20 mm cubic PM). Field uniformity and average field is calculated for 10 mm DSV. Shim piece is a 5 mm cubic PM ($\rho = 7.52 \text{ g/cm}^3$). Gap for double Halbach ring is 13 mm. $*\omega = \gamma B = 2\pi f$ and γ is gyromagnetic ratio; for glycerin: $\gamma = 2.675 \times 10^8 \text{ rad/s}$. Based on Figure 7, shim ring is inserted inside the main ring (two nested ring). Main Ring (MR), Shim Ring (ShR), number of main cubic PM (n), number of shim cubic PM (n_{sh}), same dipole (shR^+), opposite dipole (shR^-).

Configuration	Number of rings and n	r_{in} (mm)	Length (mm)	Field uniformity in ROI (ppm)	Average field strength in ROI (mT)	\mathfrak{R}	f^* (MHz)	Mass (g)
MR	1, $n = 2$	25	20	388552	66.04	0.046	2.811	120.32
MR + gap + MR	2, $n = 2$	25	53	156549	71.16	0.031	3.029	240.6
MR + ShR ⁻	2, $n = 2$	20	20	269539	51.05	0.045	2.173	127.84
2 (MR + ShR ⁻) + gap	4, $n = 2$	20	53	90865	62.51	0.041	2.661	255.7
4 main	1, $n = 4$	25	20	157176	106.25	0.046	4.523	240.64
MR + gap + MR	2, $n = 4$	25	53	71079	126.76	0.030	5.396	481.3
MR + ShR ⁻	2, $n = 4$	20	20	126606	82.46	0.039	3.510	255.68
2 (MR + ShR ⁻) + gap	4, $n = 4$	20	53	28713	108.66	0.057	4.626	511.4
MR	1, $n = 6$	25	20	86684	153.43	0.053	6.532	360.96
MR + gap + MR	2, $n = 6$	25	53	38485	194.10	0.038	8.263	721.92
MR + ShR ⁻	2, $n = 6$	20	20	112239	121.17	0.029	5.158	383.5
2 (MR + ShR ⁻) + gap	4, $n = 6$	20	53	8091	163.13	0.1348	6.945	767
MR + ShR ⁺	2, $n = 12$, $n_{sh} = 4$	27.5	20	39158	132.820	0.019	5.654	736.96

$$r_{in} = r_d \left(1 - \sin\left(\frac{\pi}{n}\right)\right),$$

$$\text{for cubic: } r_{in} = r_d \left(1 - \sqrt{2}E(\alpha)\right), \quad (8)$$

$$r_{out} = r_d \left(1 + \sin\left(\frac{\pi}{n}\right)\right),$$

$$\text{for cubic: } r_{out} = r_d \left(1 + \sqrt{2}E(\alpha)\right), \quad (9)$$

$$a = 2r_d \sin\left(\frac{\pi}{n}\right)$$

$$\text{for cubic: } a = 2r_d E(\alpha), \quad (10)$$

and:

$$E(\alpha) = \left[\cos(\alpha) - \sin(\alpha) - \sqrt{2} \sin(\pi/4 - 2\alpha) \right] / \left[2\cos(\pi/4 - 2\alpha) + \sqrt{2} \right], \quad (11)$$

$$B = B_r l n \frac{r_{out}}{r_{in}}. \quad (12)$$

3. Simulation results

In the following, different Halbach configurations are considered and they are simulated using the Maxwell software.

3.1. Circular cross-section PM

When $n = 4$, $r_{in} = 21.5 \text{ mm}$, rd , r_{out} and a are calculated using Eqs. (8)–(10) and they are 73.4 mm, 125.3 mm and 103.8 mm, respectively. Figure 2 displays the magnitude and polarity for four cylindrical PM column. In Maxwell, NdFeB35 (sintered type) is selected as a PM material and its B_r is set to 1.223 T (for bonded type this value is 0.65 T which is not used here) which is different from average value 0.79 T measured on the surface of PM piece ($r_{PM} = 7.5 \text{ mm}$, $l_{PM} = 25 \text{ mm}$). This is because the maximum value of B_r is used in the magnet physical data table and equations in the software. There is a gap between two Halbach rings. This gap has been considered for increasing the homogeneity of magnetic field density. In Figure 3, the magnetic field density versus gap is simulated. Compared with 0 mm gap, it is seen

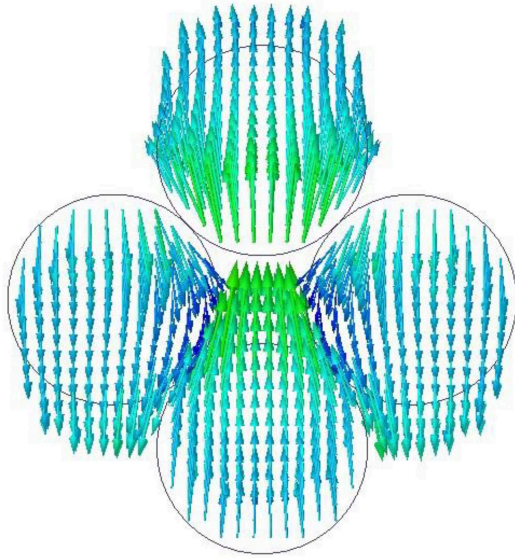


Figure 2. The direction of magnetic field density.

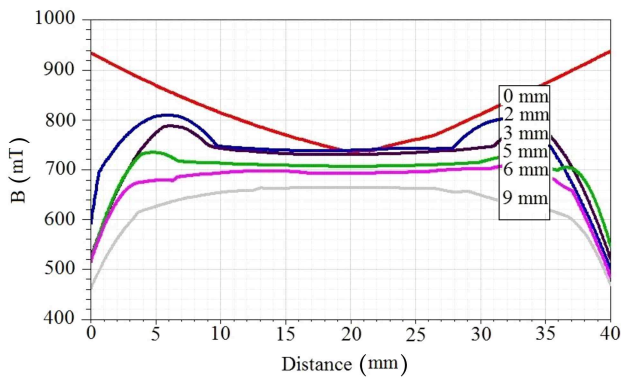


Figure 3. The changes of distribution of magnetic field density along with Halbach polarity versus changes of gap distance between two rings.

that the gap inhomogeneity has decreased at 3 mm. With increasing the gap, homogeneity is increased at first and it is then decreased. When the ideal Halbach magnet (with infinitely length and donut ring) is designed, Eq. (11) is used. For example, $B = 0.418$ T and $B_r = 0.79$ T, from Eq. (8), Eq. (9) and Eq. (12), $n = 15$ are obtained. We select $n = 12$ and $a = 15$ mm. Then, $r_d = 29$ mm, $r_{out} = 36.5$ mm and $r_{in} = 21.5$ mm. For these dimensions, the polarity is shown in Figure 4. In Maxwell software, this material polarity is added based on α_i , β_i for each column. The magnetic field is decreased because ideal magnet (infinitely length and donut ring) is not designed here ($l = 50$ mm + Gap). For this configuration, axial shimming is analyzed. In Figure 5, the homogeneity and B_{avg} of ROI (with 10 mm diameter of spherical volume (DSV)) versus the height of Halbach ring is shown. Based on [27], $L_1/r = 0.46$ and $L_2/r = 0.91$ are considered here, where L_i is axial distance from center of layers

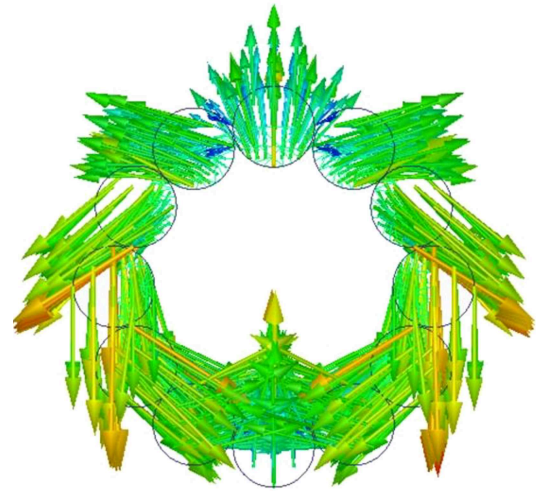


Figure 4. The direction of magnetic field density.

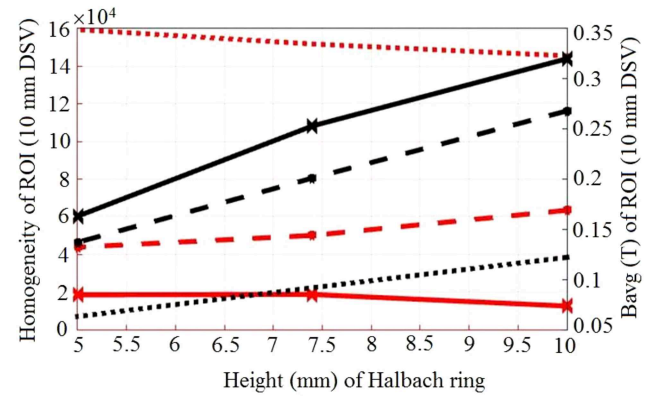


Figure 5. The inhomogeneity and B_{avg} related to ROI (with 10 mm DSV) versus height of Halbach ring (with 12 pcs). Solid line: Five layer, Dash line: Three layer, Dotted line: One layer.

to the origin of coordinates. Here, $L_1 = 13.34$ mm and $L_2 = 26.39$ mm. Then, the axial position of ring layers from central layer is determined by L_i . When H is height of Halbach ring, $HGap_1HGap_1H$ and $HGap_2HGap_1HGap_1HGap_2H$ are selected for three layers and five layers, respectively. And, 10 mm DSV lines are selected on x -axis, y -axis, z -axis, $y = x = z$, $y = -x = z$, and $y = x = -z$.

3.2. Cubic PM pieces and shimming

1. Minimum stray field: The frame should be made from aluminum or polyvinyl chloride (PVC) or thick PMMA. Halbach ring is made based on Eqs. (8)-(11). In Figure 6, for $n = 12$ and $a = 20$ mm, we have $r = 45.71$ mm, $r_{in} = 31.56$ mm, $r_{out} = 59.85$ mm which is figured in AutoCAD (inner ring is for shimming). For $n = 16$ and $a = 10$ mm, we have $r = 31.54$ mm, $r_{in} = 24.47$ mm, $r_{out} = 38.61$ mm. This structure results in better uniformity.
2. Maximum frame strength: Regarding the proposed

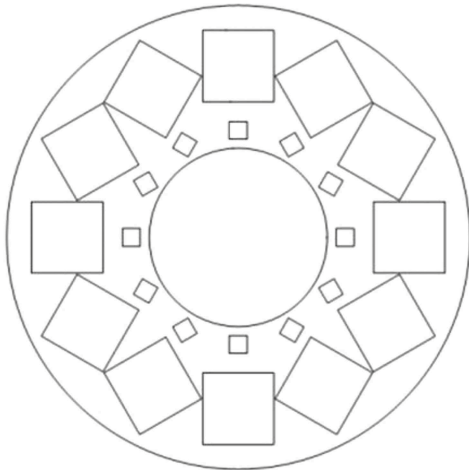


Figure 6. The Halbach ring with minimum stray field.

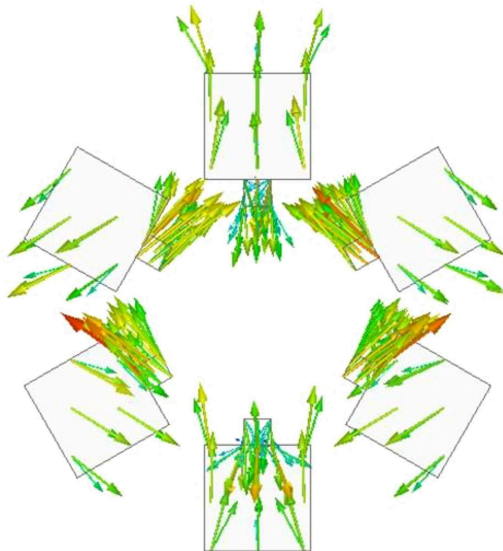


Figure 7. The direction of magnetic field density where main Halbach ring is outer ring and the shimming Halbach ring is inner ring and $n = 6$.

idea, it is easy to install the PM pieces, especially if the frame is made of PMMA, PLA, and wood. Main Halbach rings with 2 pcs, 4 pcs, and 6 pcs (for $a = 20$ mm) are separately placed along with 25 mm radius circle. Direction of magnetic field density is shown in Figure 7. Inner shimming Halbach ring with 2 pcs, 4 pcs, and 6 pcs (for $r_{in} = 25$ mm) are polarized with inverse direction. In Figure 8, shimming ring effect on the homogeneity is shown. Clearly, the homogeneity is increased based on the solid lines. The volume of main PM piece should be greater than shimming PM piece volume. Then, the number of shimming pieces should be equal with or greater than main PM pieces. When the number of shimming PM pieces is changed, Figure 9 shows homogeneity and average field (12 pcs, main ring,

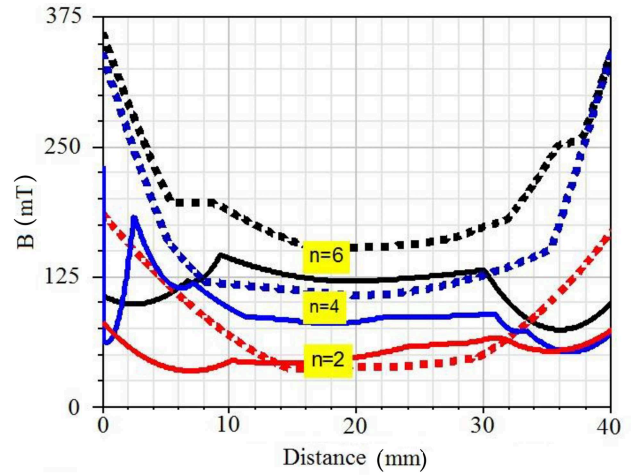


Figure 8. Distribution of magnetic field density along with Halbach dipole direction (for $n = 2, 4,$ and 6). Dot line: main Halbach ring. Solid line: main Halbach ring with shimming Halbach ring.

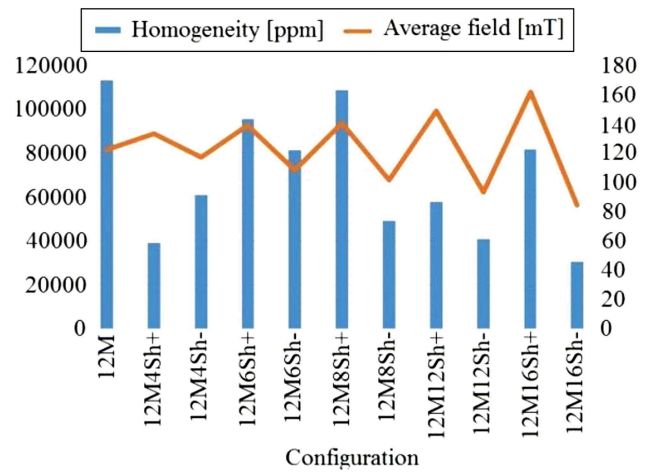


Figure 9. Homogeneity and average field versus configuration (for $n = 12, n_{sh} =$ variable).

sh^+ for same polarity; sh^- for opposite polarity). Therefore, two nested rings (main and shimming) should be used. Depending on the amount of non-uniformity and the number of magnet pieces, the best structure can be selected with regard to Figure 9. Here, the ring with 12 pieces of PMs is selected to produce. Different configurations and various design parameters are considered and average field and homogeneity determined for them are summarized in Table 1. As clear from this table, the inhomogeneity is decreased when the number of PM pieces is increased.

3.3. Regular polyhedron cross-section and radial shimming

In [14], regular polyhedron PM was used and acceptable results were reported. For each hexagonal, side size = 57 mm, height = 50 mm, usable gap = 100 mm

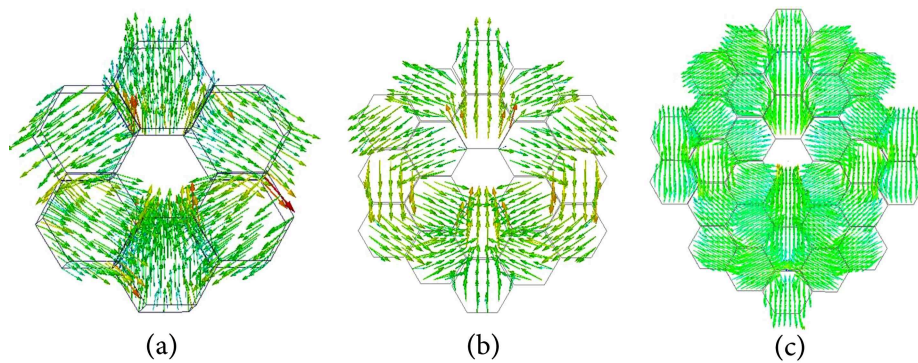


Figure 10. The direction of magnetic field density: (a) for one ring (composed of 6 pcs regular polyhedron PM pieces), (b) for two layers (two nested rings) with 18 pcs, and (c) for three layers (32 pcs).

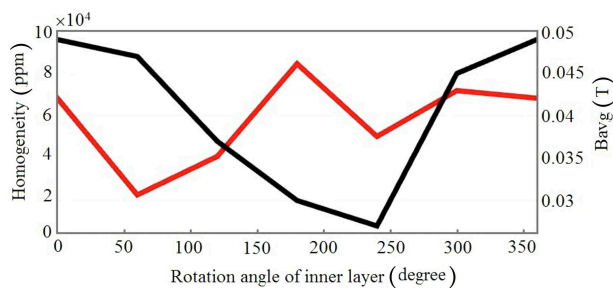


Figure 11. The homogeneity and average magnetic field density versus rotation angle of inner ring for two nested ring.

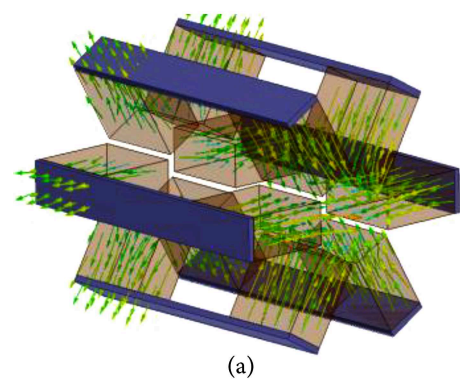
and directions of magnetic field density are shown in Figure 10. In Figure 10(c), shimming PM pieces are illustrated based on their magnetic directions. In Figure 11, homogeneity and average are compared. The minimum of η and B_{avg} has occurred at 60° and 240° , and its figure of merit is $\mathfrak{R} = 0.00002$ (T/kg). As seen, this configuration has a low magnetic field and high weight, and therefore it is not acceptable for large scale dimensions.

3.4. Shimming U-shaped magnet by Halbach array

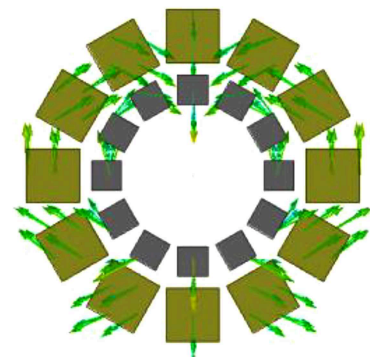
Here, U-shaped and Halbach magnet units are combined to obtain homogenous magnetic field density in the ROI. U-shaped magnet, two-layer Halbach magnet, and combined magnet are shown in Figure 12(a), Figure 12(b), and Figure 13, respectively. The effect of combination is shown in Figure 14. With regard to the U-shaped curve depicted in Figure 14, the field has decreased in the position of U-shaped PMs and it is increased between them. Nevertheless, another decline has occurred between them. To compensate this, five Halbach rings (12 cubic pieces in each ring) are installed inside the U-shaped ring.

4. Experimental results

The average remanence field value is measured on



(a)



(b)

Figure 12. The considered topology: (a) U-shaped magnet (inner radius is 25 mm) (b) two-layer Halbach magnet (inner radius is 25 mm).

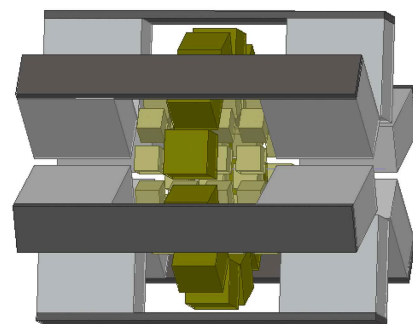


Figure 13. The combined structure.

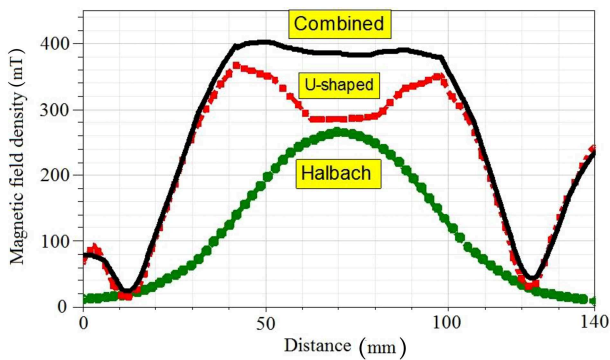


Figure 14. Optimization of magnetic field homogeneity.

the pole surfaces of 2 mm cube. This field is not fixed at different points (average value: 450 mT). The frame is made from PMMA by laser cutter (model: crystal). PMMA is more expensive, fully transparent, and friendly with environment. Other materials (such as Teflon family (PLA, polyamide, poly ethylene ...), PVC, wood, aluminum ...) are fully opaque. AutoCAD output file should be saved as *.dxf file to be opened in work laser software. In Figure 15, PMMA and PVC frames ($n = 12$) are made first ($r_{in,frame} = 25$ mm, $r_{out,frame} = 65$ mm). Aluminum frame was made from PVC frame as a casting mold in the casting workshop. Figure 15(d) shows PVC

frame for $n = 16$. In Figure 15(e), pliers have been used to install magnet pieces. Figure 15(f) depicts the created ring for radially shimming; the main ring (12 cubic PM, $a = 20$ mm, $r_{in} = 33.1$ mm, $r = 48$ mm, $r_{out} = 62.8$ mm) and shimming ring (4 column, $a = 5$ mm, $h = 20$ mm, $r_{in,sh} = 27.5$ mm and $r_{out,sh} = 32.5$ mm). The bipolar fields produced by two rings are aligned. The magnet height is placed from $z = 0$ to $z = 20$ mm (cylindrical axis is placed on Z -axis). In Table 2, the average field and homogeneity have been summarized. Tesla measurement (in 10 mm DSV) is done by Lutron (model MG-3002). In Figure 15(f), Halbach magnet with 6 rings ($n = 16$, $a = 10$ mm, $r_{in} = 26.4$ mm, $r = 34$ mm, $r_{out} = 41.6$ mm) is made. Then, axial shimming is researched for multiple layers and distances. In Table 3, some tests for this magnet are inserted. Here, two, four and six rings (even number not odd number) are used. The best distance is achieved via trial-and-repeat as well as simulation. It should be explained that m_L specifies the number of layers and L_1 , L_2 , and L_3 are the distance between the pairs of the first layer, the distance between the pairs of the second layer and the distance between the pairs of the third layer, respectively. However, the homogeneity will be changed when the sampling is done more precisely.

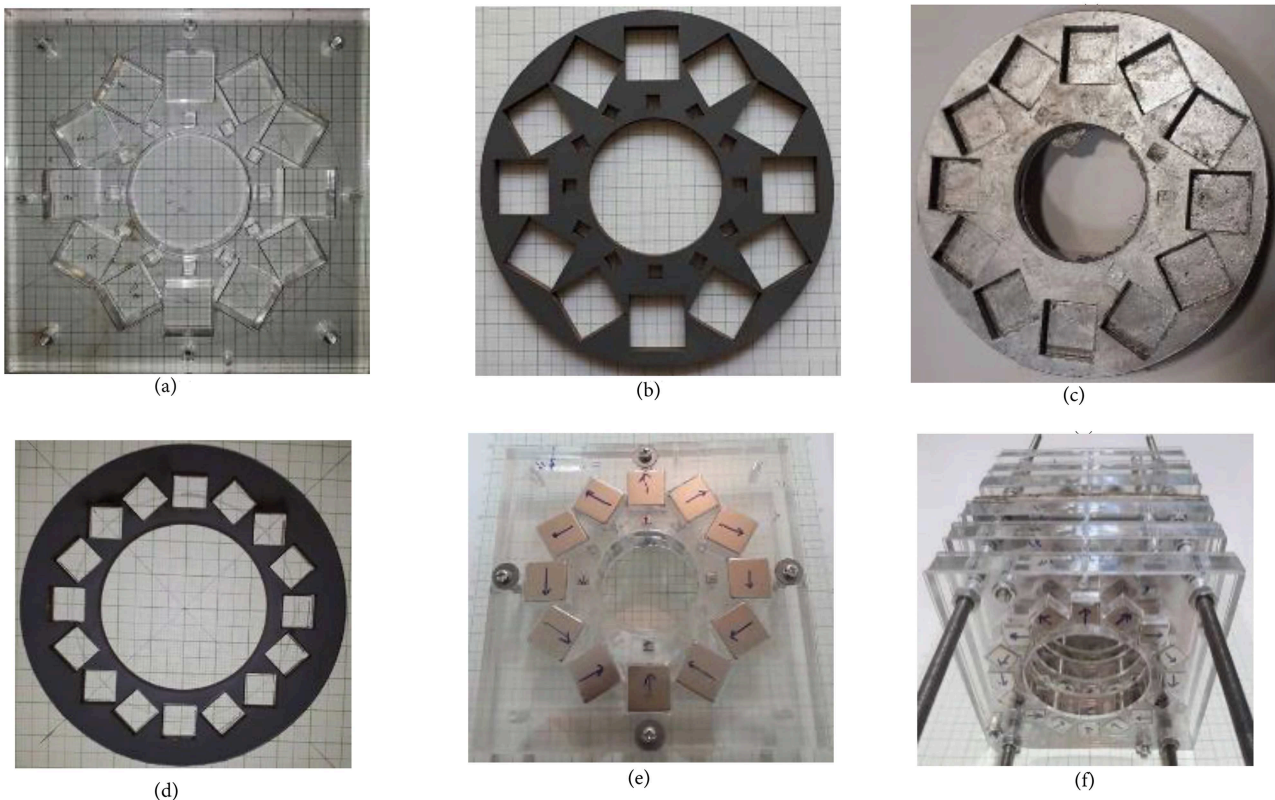


Figure 15. Different structures: (a) PMMA frame for $n = 12$, $n_{sh} = 12$, (b) PVC frame for $n = 12$, $n_{sh} = 12$, (c) Aluminum frame for $n = 12$ (without shimming slots), (d) PVC frame ($n = 16$), (e) produced magnet for radial shimming method ($n = 12$, $n_{sh} = 4$), and (f) produced magnet for axial shimming method ($n = 16$, 6 rings).

Table 2. Measurement of homogeneity and average field (radial shimming, $n = 12$, $a_m = 1220$ mm, $a_{sh} = 5$ mm, $n_{sh} = 4$).

	Average field (mT)		Homogeneity (ppm)	
	Main magnet	Shimmed magnet	Main magnet	Shimmed magnet
$z = -3$ mm	95.34	100.92	24123	7926
$z = 10$ mm	113.38	120.87	22050	29784
$z = 20$ mm	101.38	108.04	20715	19436

Table 3. Measurement of homogeneity and average field for even number rings (axial shimming, $n = 16$, $a = 10$ mm).

	Average field (mT)		Homogeneity (ppm)	
	Measured	Simulated	Measured	Simulated
$m_L = 2$, $L_1 = 21$ mm	46.48	46.59	62968	72587
$m_L = 4$, $L_1 = 16$ mm, $L_2 = 36.5$ mm	81.28	79.06	405684	51805
$m_L = 6$, $L_1 = 15$ mm, $L_2 = 35$ mm, $L_3 = 52$ mm	91.15	90.50	29622	42751
$m_L = 6$, $L_1 = 11$ mm, $L_2 = 32$ mm, $L_3 = 47$ mm	117.63	108.83	3400	7432

5. Summary and conclusion

The main equations related to the Halbach magnet design were obtained at first. Then, different structures for Halbach magnet were simulated by Maxwell software. Considering different configurations, radial and axial shimming methods were analyzed via trial and error and the best structure was selected. The average field and homogeneity as performance factors were used to evaluate the magnets. The supporting frame was produced by Crystal laser from Poly Methyl Metha Acrylate (PMMA) material. Practically, the axial and radial shimmed Halbach magnets were made by installing PM pieces on the frame. Based on the obtained simulation and experimental results, it was seen that the generated Halbach magnets were acceptable for a low-field portable Magnetic Resonance Imagine (MRI) system. As a future work, optimization algorithms could be used to find better result for the optimized topology.

References

- Shiravi, M., Ganji, B., and Shiravi, A. "Static coil design considerations for the magnetic resonance imaging", *International Journal of Engineering*, **32**(3), pp. 393–399 (2019). DOI: 10.5829/ije.2019.32.03c.06
- Halbach, K. "Strong rare earth cobalt quadrupoles", *IEEE Transactions on Nuclear Science*, **26**(3), pp. 3882–3884 (1979). DOI: 10.1109/TNS.1979.4330638
- Marques, J.P., Simonis, F.F.J., and Webb, A. "Low-field MRI: An MR physics perspective", *Journal of Magnetic Resonance Imaging*, **49**(6), pp. 1528–1542 (2019). DOI: 10.1002/jmri.26637
- Vos, B., Fuchs, P., O'Reilly, T., et al. "Gradient coil design and realization for a Halbach-based MRI system", *IEEE Transactions on Magnetics*, **56**(3), Art no. 5100208 (2020). DOI: 10.1109/TMAG.2019.2958561
- O'Reilly, T., Teeuwisse, W.M., and Webb, A.G. "Three-dimensional MRI in a homogenous 27 cm diameter bore Halbach array magnet", *Journal of Magnetic Resonance*, **307**, 106578 (2019). DOI: 10.1016/j.jmr.2019.106578
- Itasaka, T., Ishiguro, Y., Shinozaki, K., et al. "Investigation of magnetic performance on the cylinder-shaped PM type linear Halbach array assembled by 45 degree rotating arrangement", *12th International Symposium on Linear Drives for Industry Applications*, Switzerland, pp. 1–6 (2019). DOI: 10.1109/LDIA.2019.8771000
- Nakagomi, M., Kajiwara, M., Matsuzaki, J., et al. "Development of a small car-mounted magnetic resonance imaging system for human elbows using a 0.2 T permanent magnet", *Journal of Magnetic Resonance*, **304**, pp. 1–6 (2019). DOI: 10.1016/j.jmr.2019.04.017
- Cooley, C.Z., Haskell, M.W., Cauley, S.F., et al. "Design of sparse Halbach magnet arrays for portable MRI using a genetic algorithm", *IEEE Transactions on Magnetics*, **54**(1), Art no. 5100112 (2018). DOI: 10.1109/TMAG.2017.2751001
- Chen, J., Wang, D., Cheng, S., et al. "A hysteresis model based on linear curves for NdFeB permanent magnet considering temperature effects", *IEEE Transactions on Magnetics*, **54**(3), Art no. 2100505 (2018). DOI: 10.1109/TMAG.2017.2763238
- Huang, H., Jing, L., Qu, R., et al. "Analysis and application of discrete Halbach magnet array with unequal arc lengths and unequally changed magnetization directions", *IEEE Transactions on Applied Superconductivity*, **28**(3), Art no. 5201305 (2018). DOI: 10.1109/TASC.2017.2785399

11. O'Reilly, T., Teeuwisse, W.M., Gans, D., et al. "In vivo three-dimensional brain and extremity MRI at 50 mT using a permanent magnet Halbach array", *Magnetic Resonance in Medicine*, **85**(1), pp. 495–505 (2020). DOI: 10.1002/mrm.28396
12. Phuc, H.D. "Development of portable low field NMR magnet: design and construction", PhD Thesis, Medical Imaging INSA de Lyon (2015).
13. Burgwal, R. "Measuring NMR and developing 2D imaging in a low-cost portable MRI prototype", MSc Thesis, Leiden University (2018).
14. Blümich, B., Rehorn, C., and Zia, W. "Magnets for small-scale and portable NMR", In *Micro and Nano Scale NMR: Technologies and Systems*, Anders, J., Korvink, J.G., Wiley-VCH Verlag GmbH and Co. KGaA, pp. 1–20 (2018). DOI: 10.1002/9783527697281.ch1
15. Blümmler, P. and Casanova F. "Hardware developments: Halbach magnet arrays", In *Mobile NMR and MRI*, Johns, M.L., Fridjonsson, E.O., Vogt, S.J., Haber A., Cambridge: The Royal Society of Chemistry, pp. 133–157 (2016). DOI: 10.1039/9781782628095-00133
16. Ren, Z.H., Mu, W.C., and Huang, S.Y. "Design and optimization of a ring-pair permanent magnet array for head imaging in a low-field portable MRI system", *IEEE Transactions on Magnetics*, **55**(1), Art no. 5100108 (2018). DOI: 10.1109/TMAG.2018.2876679
17. Hockx, J. "Designing and characterizing a hardware and software acquisition system for low field MRI", MSc thesis, Leiden University (2017).
18. Van, D.K. "Low field MRI using halbach ferromagnet arrays", BSc thesis, Leiden University (2017).
19. Ren, Z.H., Maréchal, L., Luo, W., et al. "Magnet array for a portable magnetic resonance imaging system", *International Microwave Workshop Series on RF and Wireless Technologies for Biomedical and Healthcare Applications*, Taiwan, pp. 92–95 (2015). DOI: 10.1109/IMWS-BIO.2015.7303793
20. Salajeghe, S. "Image encoding and reconstruction for portable magnetic resonance imaging", PhD Thesis, University of Saskatchewan (2016).
21. Breimer, W. "The measurement of an NMR signal with Halbach arrays: progressing towards low-budget MRI using permanent magnets", MSc Thesis, Leiden University (2019).
22. Purchase, A.R., Vidarsson, L., Wachowicz, K., et al. "A short and light, sparse dipolar Halbach magnet for MRI", *IEEE Access*, **9**, pp. 95294–95303 (2021). DOI: 10.1109/ACCESS.2021.3093530
23. Rajendran, M. and Huang, S.Y. "Asymmetric tapered solenoid designs for Halbach-based portable magnetic resonance imaging", *IEEE Journal of Electromagnetics, RF and Microwaves in Medicine and Biology*, **7**(1), pp. 52–58 (2023). DOI: 10.1109/JERM.2022.3213994
24. Seleznyova, K., Strugatsky, M., and Kliava, J. "Modelling the magnetic dipole", *European Journal of Physics*, **37**(2), Art no. 025203 (2016). DOI:10.1088/0143-0807/37/2/025203
25. Jayatilake, M.L. "Optimization and construction of passive shim coil for human brain at high-field MRI", PhD thesis, University of Cincinnati, USA (2011).
26. Raich, H. and Blümmler, P. "Design and construction of a dipolar Halbach array with a homogeneous field from identical bar magnets: NMR Mandhalas", *Concepts in Magnetic Resonance*, **23B**(1), pp. 16–25 (2004). DOI: 10.1002/cmr.b.20018
27. Chen, Q., Zhang, G., Xu, Y., et al. "Design and simulation of a multilayer Halbach magnet for NMR", *Concepts in Magnetic Resonance*, **45B**(3), pp. 134–141 (2015). DOI: 10.1002/cmr.b.21292

Biographies

Mohammadreza Shiravi was born in Esfahan, Iran, on December 1, 1984. He received the BSc degree in electrical engineering from Shahrekord University, Iran, in 2009. He received the MSc degree from Tafresh University, Iran, in 2014 and PhD degree in 2021 from University of Kashan, Iran. His special field of interest is design of electric machines and MRI system.

Babak Ganji received BSc degree from Esfahan University of Technology, Iran in 2000, and MSc and PhD from University of Tehran, Iran in 2002 and 2009 respectively, all in major electrical engineering-power. He was granted DAAD scholarship in 2006 from Germany and worked in institute of power electronics and electrical drives at RWTH Aachen University as a visiting researcher for 6 months. He has been working at University of Kashan in Iran since 2009 as an associate professor and his research interest is modeling and design of advanced electric machines especially switched reluctance motor.